ELSEVIER

Journal of Marine Systems 20 (1999) 279–300

JOURNAL OF MARINE SYSTEMS

Modeling dense water mass formation and winter circulation in the northern and central Adriatic Sea

Andrea Bergamasco [a,*], Temel Oguz [b], Paola Malanotte-Rizzoli [c]

[a] *Istituto per lo Studio della Dinamica delle Grandi Masse (ISDGM)-CNR 30125 Venice, 1264 S. Polo, Italy*
[b] *Institute of Marine Sciences, METU, Erdemli, Turkey*
[c] *Department of Earth, Atmospheric and Planetary Sciences, MIT, Cambridge, MA, USA*

Received 10 August 1997; accepted 20 December 1997

Abstract

In this paper, using an eddy resolving primitive equation model, we attempt to provide quantitative answers to some of the still unresolved or poorly understood dynamical issues related to the general circulation of the northern and central Adriatic Sea. The first question we addressed relates to understanding the effects of the major driving mechanisms on the basin circulation. A series of numerical experiments are carried out to examine the circulation produced by various combinations of different forcing mechanisms. Cold air outbreaks (CAO) associated with the northeasterly bora winds, together with uniform surface cooling and freshwater discharge prescribed near the northwestern corner, give a fairly realistic circulation consistent with the observations. This pattern is comprised of an overall cyclonic gyre in the northern basin, with a strong southward flowing jet along the Italian coastline and a broader northward flow along the Croatian coast. The second question addressed is under what conditions convective mixing extends to the bottom of the Jabuka Pit. While the northern shelf is always uniformly mixed to the bottom, the extent of convection within the Pit depends on the overall stratification prior to onset of the CAO event. Strong subsurface stratification between the intermediate and near-bottom layers prevents deep convection. The third question concerns with the role of the rim current along the Italian coast vs the other circulation components in distributing the North Adriatic Dense Water (NADW) within the basin. In general, the strong density front developed across the shelf break north of the Jabuka Pit restricts the replenishment of the Pit deep layers by the NADW. Rather, the NADW is transported southward along the Italian continental slope in the form of a vein of underflow. The final question addressed is how the thermohaline structure of the water column evolves after the ending of the CAO event, and of the related convection process.

Keywords: winter circulation; Adriatic Sea; cold air outbreaks (CAO)

1. Introduction

Even though marginal in the configuration of the Mediterranean basin, the Adriatic Sea (Fig. 1a) has the unique feature of being the site of two different water mass formation process according to the classification given by Killworth (1983). The first one is the wintertime Northern Adriatic Dense Water (NADW) mass formation process occurring in the northern half of the basin over the continental shelf of ~ 500 km long, and near the shelf break. Thus,

* Corresponding author. Fax: +39-041-2602340; E-mail: andreab@isdgm.ve.cnr.it

PII: S0924-7963(98)00087-6

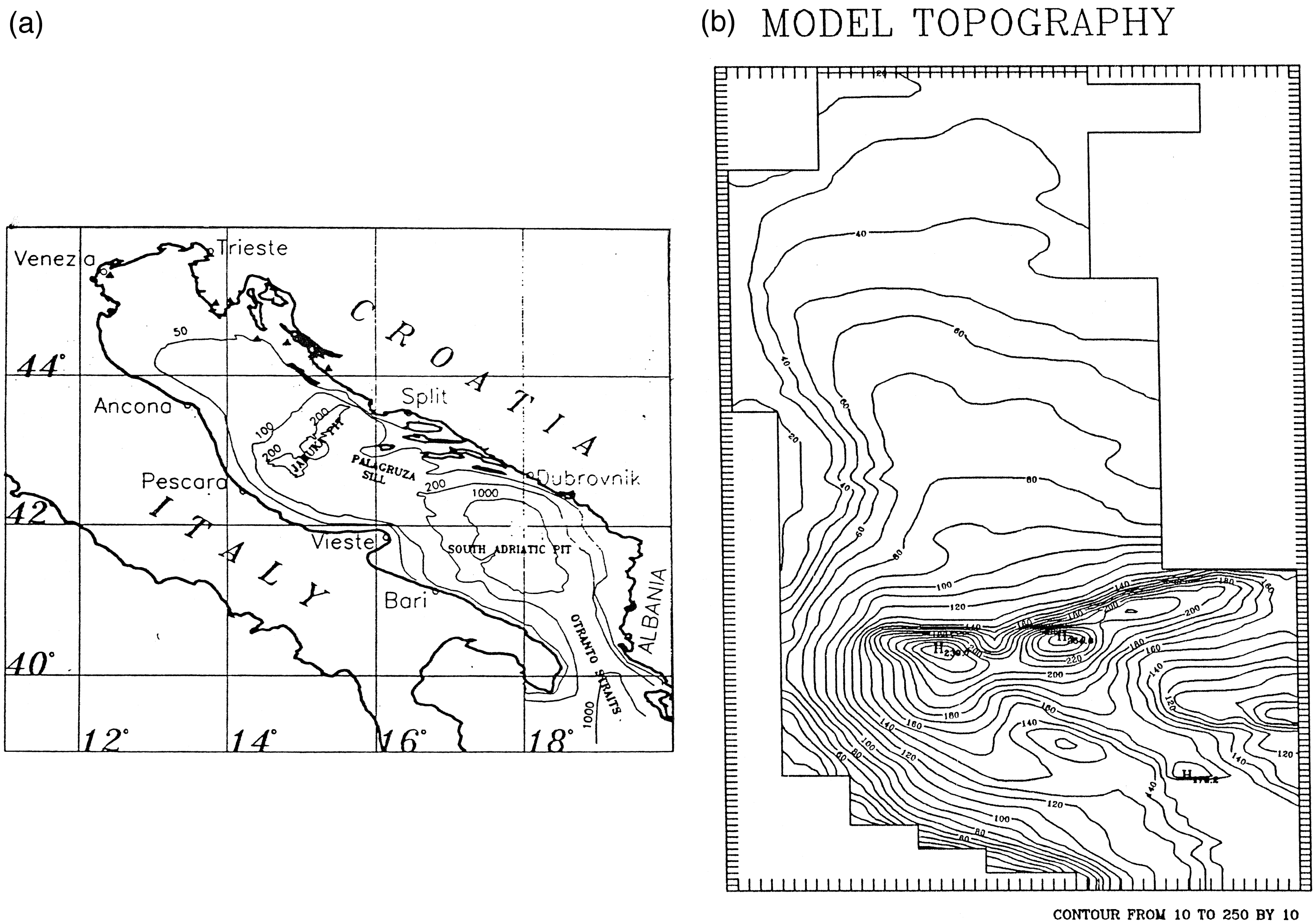

Fig. 1. (a) The location map and bathymetry of the Adriatic Sea. (b) Model domain and topography.

the northern Adriatic can be considered as a prototype for this kind of water mass formation process (Malanotte-Rizzoli, 1991) that has been documented in a series of investigations (Hendershott and Rizzoli, 1976; Artegiani and Salusti, 1987; Artegiani et al., 1989). The second type of process is open ocean deep convection which seems to occur in the southernmost part of the basin, reaching ~1200 m depth (Ovchinnikov et al., 1985). This water mass outflows at depths from the Otranto Strait (Pollak, 1951) and drives the entire Eastern Mediterranean deep thermohaline circulation (Roether and Schlitzer, 1991; Schlitzer et al., 1991).

The observed yearly-averaged circulation of the Adriatic Sea is characterized by an overall cyclonic circulation (Malanotte-Rizzoli and Bergamasco, 1983; Orlic et al., 1992; Artegiani et al., 1993) consisting of two permanent gyres. The first gyre covers the southern deep basin and is isolated from the northern part by the Palagruza Sill. The second cyclonic gyre is situated over the northern shallow shelf and the Jabuka Pit region of the central basin. The mean circulation possesses seasonal variability in response to changing winds and thermal fluxes during the year. The winter circulation is driven by a combination of relatively weak but persistent southeasterly winds (the so-called scirocco), the surface thermohaline fluxes and short term episodes of the strong northeasterly winds (the so-called bora) associated with the cold air outbreaks from the continent. Along the northwestern side of the basin the fresh water outflow, mostly originating from the River Po, also contributes to the circulation even though its contribution is not as pronounced as in the spring and summer period (Hendershott and Rizzoli, 1976). The relative importance of these individual mechanisms in driving the basinwide circulation system and in modifying the local circulation features is not yet well understood.

Numerical modeling studies for the Adriatic Sea are in fact surprisingly few, simplistic and far from providing an overall dynamical framework for the basin's circulation and thermohaline structure. Kuzmic et al. (1985), Bone (1993), and Orlic et al. (1994) have described the bora and scirocco induced circulations without considering other driving mechanisms. The work of Malanotte-Rizzoli and Bergamasco (1983), on the other hand, was limited to the coastal region of the northern Adriatic affected by the fresh water discharges. Their concern was essentially to understand the regional dynamics in relation to the eutrophication process and material transport. The old idealized model of Hendershott and Rizzoli (1976) appears to be the only modeling study relevant for studying the winter thermohaline structure and related NADW formation in the northern basin under the combined forcings by the freshwater discharge, wind and surface cooling. The Adriatic Sea is recently subjected to intensive interdisciplinary modeling studies (Pinardi, 1995).

In the shallow northern shelf region and its extension to the central basin, the NADW is formed in winter during the outbreaks of the cold and dry bora winds that induce strong evaporation and cooling. It is characterized by a wide range of T, S characteristics of 9–12°C and 38.1–38.4 ppt, depending on the regional and meteorological characteristics (Hendershott and Rizzoli, 1976; Artegiani and Salusti, 1987). This dense water mass is known to flow southwards along the isobaths of the Italian continental shelf and slope at depths of 50–150 m (Artegiani et al., 1989), and exits from the Otranto Strait into the Ionian Sea (Bignami et al., 1990). Details of the evolutionary characteristics of this coastal underflow is, however, poorly understood. A quantitative dynamical description of the associated processes is not yet available.

In the topographically controlled cyclonic gyre of the southern basin, the deep open ocean convection to depths of about 750 m (Ovchinnikov et al., 1985) generates the Adriatic Bottom Water (ABW). It is mainly formed by mixing of the surface waters of Ionian origin with the relatively warmer (~14°C) and more saline (~38.5–38.7 ppt) waters of the Modified Levantine Intermediate Water mass (MLIW) entering into the region at intermediate depths of 200–400 m along the eastern part of the Otranto Strait. The NADW transported southwards as a vein of dense underflow also contributes to this process through its mixing with the local subsurface waters.

While the formation of the dense water mass in the southern Adriatic Pit is identified to a certain degree by the hydrographic observations, the vertical extent of the deep convection in the cyclonic gyre encompassing the Jabuka Pit of the central Adriatic

(Paschini et al., 1993) is not well documented from in situ data. The convective overturning process limited to the upper 100 m is reported to occur here regularly as on the northern Adriatic shelf. The penetration of convection all the way to the bottom of the pit ($\sim$ 250 m) is, however, not clear from the observations, and does not seem to be repeating regularly every winter. In addition to the intensity of winter cooling, the stratification characteristics of the intermediate and deep water masses generated by the interaction of warmer and saltier MLIW and the colder and fresher NADW prior to the winter convection may play a very important role in the dense water mass characteristics of the central basin.

The objective of the present work is to provide a dynamical framework to understand the role of different driving mechanisms in producing the observed circulation features. Using an eddy resolving primitive equation general circulation model with fairly idealized representation of the northern Adriatic geometry and bottom topography, a hierarchy of numerical experiments with different level of complexity in their forcing is carried out to explore the individual contributions of the scirocco and bora winds, the surface and lateral buoyancy fluxes on the winter circulation and thermohaline structure of the northern Adriatic. We specifically attempted to clarify some questions raised from the observational studies but still lack quantitative explanation up to now. We address the following four major questions: (i) What are the effects of major driving mechanisms (different wind stress fields, thermal flux and river discharge) on the basin circulation, and which ones are crucial in providing the observed circulation pattern? (ii) Under what conditions can the convection extend to the bottom of the Jabuka Pit? (iii) What are the relative contributions of the rim current flowing southward along the Italian coast and the other components of the circulation system in distributing the dense water mass formed in the northern shallow basin? (iv) How does the thermohaline structure of the water column evolve after the cooling weakens and convection ceases?

The formulation of the model is presented briefly in Section 2. Section 3 describes the specific model simulations. The discussion of the results and a summary of the important findings are given in Section 4.

2. Model description

The model used is the Princeton Ocean Model described by Mellor (1990). It is a three dimensional, f-plane, free surface primitive equation model for an incompressible, Boussinesq and hydrostatic fluid employing the bottom—following sigma coordinate system in the vertical. It includes an active thermodynamics and the order 2.5 turbulence closure scheme for the parameterization of vertical mixing (Mellor and Yamada, 1982). The prognostic equations are those for the horizontal velocity components, temperature and salinity, the turbulent kinetic energy and the turbulence macroscale. These turbulence quantities together with the vertical velocity shear and buoyancy are used to determine the vertical mixing coefficients for momentum and thermodynamic variables. Therefore, no convective adjustment mechanism is invoked, and the unstable conditions in the stratification is removed by the intensified vertical mixing obtained through the turbulence parameterization. In the context of general circulation studies, application of the model to the Mediterranean and Black Sea basins are given by Zavaterelli and Mellor (1995), and Oguz et al. (1995), respectively.

The model resolves the vertical stratification using 15 vertical levels on the sigma coordinate system. The vertical levels are compressed towards the surface and the bottom in order to represent the boundary layer structures more properly. The geometry and the bottom topography of the basin are modeled in an idealized way by retaining only the major features, without including a fully realistic coastline and topography representation. This approach should be adequate and justifiable for this kind of process-oriented study. Their more realistic treatment is however essential in nowcasting and forecasting oriented simulations of the general circulation. Major features of the bottom topography incorporated in the model are the gently sloping isobaths along the main axis of the basin from 20 m near the northern coast to about 100 m slightly north of the latitudinal off Pescara. Thereafter, the steep topographic slope connects the northern basin to the two interconnected pits of the central basin centered along the Pescara. The Jabuka Pit has a maximum depth of $\sim$250 m and only limited communication with the southern basin via the 150 m deep mid-basin ridge, crossing the Pelagruza Sill. Along the western coast, the isobaths running parallel to the shoreline deepen rapidly over a distance of about 25 km. The southern open boundary is located along the latitudinal off Vieste, which borders the rapidly varying topography of the deep southern Adriatic. These features of the model geometry are shown in Fig. 1b.

The model considers a horizontal grid of 3.75 km in both directions, which adequately resolves the mesoscale features of the basin. This choice of grid structure requires to set the external mode time step to 15 s, whereas the internal mode time step is taken as 900 s.

2.1. Boundary conditions

An extensive number of numerical experiments is carried out with different choices of the open boundary conditions to identify their response on the regional circulation characteristics. The following is considered to be the optimal choice for this problem. Along the open boundary, free radiation conditions are applied for the normal component of the horizontal velocity for both the external and the internal modes. During outflow conditions, the temperature and salinity along the boundary are updated by their upstream values using a simplified horizontal advection equation. During inflow conditions, the horizontal advective changes of temperature and salinity across the boundary are set to zero, which allows updating the boundary values from their values at the previous time step. Intrusions from the southern basin with different T, S characteristics are therefore avoided, and the central Adriatic water mass formation process is decoupled from that of the southern basin. We thus concentrate only on the circulation and water mass characteristics developed in response to the processes in the northern/central basin. The inclusion of the southern basin's effect through an appropriate application of the open boundary conditions is extremely difficult. Prescription of T, S values representative of the southern Adriatic at the boundary at inflow conditions generates strong gradients across the boundary at the times of dense water mass formation within the model domain and therefore leads to unrealistic flow structure near the open boundary of the model.Of course, the most natural way of incorporating the effect of southern Adriatic is to extend the model further south to the Otranto Strait and to allow exchanges with the Ionian Sea through specification of appropriate boundary conditions.

2.2. Initial conditions

The model is initialized with horizontally uniform temperature and salinity profiles shown in Fig. 2. The continuous profiles with the circles represent the autumn conditions given in the POEM1 and POEM3 data (Artegiani et al., 1993). At the surface, there is a relatively warmer (~ 15°C) and fresh (~ 38.4 ppt) mixed layer of about 40 m, overlying slightly saltier

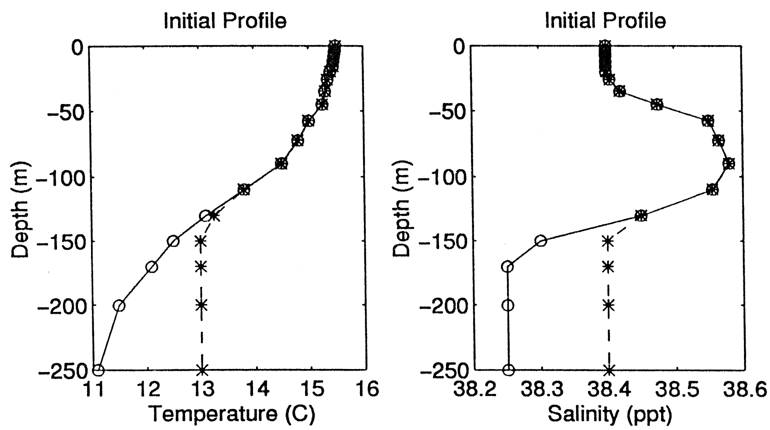

Fig. 2. Initial temperature and salinity stratifications used in the model. The continuous line represent the 'type 1' profiles, and the broken line the 'type 2' profiles.

Table 1
The list of numerical experiments

Exp. No.	Wind	Cooling	$(E-P)$	Discharge	Initial Stratification
1	Scirocco 0.5 dyn/cm^2	0	0	0	Type 1
2	0	80 W/m^2	3 mm/day	0	Type 1
3	Scirocco 0.5 dyn/cm^2	80 W/m^2	3 mm/day	0	Type 1
4	Scirocco 0.5 dyn/cm^2	80 W/m^2	3 mm/day	1500 m^3/s	Type 1
5	Temporally variable	Temporally variable	3 mm/day	1500 m^3/s	Type 1
6	Temporally variable	Temporally variable	3 mm/day	1500 m^3/s	Type 2

($\geq$ 38.5 ppt) and cooler water of Mediterranean origin extending to a depth of about 120 m. At a deeper over the Jabuka Pit, this typical shelf stratification is modified by the presence of relatively cold (11–13°C and fresh 38.25 ppt) water representing a remnant of NADW formed in previous winters in the northern Adriatic. The profiles shown by the broken lines with the stars in Fig. 2 represent the other extreme case of relatively warmer ($\sim$ 13°C) and saltier ($\sim$ 38.4 ppt) waters occupying the deepest sections of the Pit. The latter conditions are observed in the Pit under increased MLIW intrusion into the central basin and its mixing with the ambient near-bottom waters prior to the beginning of the strong cooling season.

Application of horizontally uniform initial T, S fields and adaptation of the River Po freshwater source at a single position are two other simplifications made in the model. It will be shown in the following that these choices are not critical to the model as it is able to develop realistic thermohaline structure at seasonal time scale.

3. Results

A total of six numerical experiments given in Table 1 is described here to explore the characteristics of the circulation and thermohaline structure of the northern and central Adriatic.

3.1. Circulation driven by scirocco winds

In the first experiment, the circulation is driven only by the southeasterly scirocco winds. The model is forced by the spatially uniform wind stress of 0.5 dyn/cm^2, representative of the mean conditions over the winter season. The wind stress forcing lasts a total of 60 days at which time the circulation attains a steady state. The circulation developed at 5 m depth is shown in Fig. 3a. Also included in this figure is the sea surface elevation field giving the depth averaged circulation system in the basin. The most prominent feature of the surface circulation is the presence of a pair of counter-flowing current system along the Italian coast. The narrow along-coast shelf zone is characterized by relatively stronger northward flowing currents, which are entering into the basin from the westernmost side of the open boundary. It deflects anticyclonically on its way along the shelf, supporting the southward flowing current system adjacent to it. While the southward current is a consequence of the dominant geostrophic balance, the northward inner shelf currents are the direct response of the wind driven Ekman transport. In the interior and eastern part of the basin, the circulation is dominated by the eastward and northeastward currents originating from the southerly flowing jet along the Italian coast. A tendency to a cyclonic circulation is evident in the shallow northern basin. As implied by the surface elevation field,

Fig. 3. (a) Steady state (day 60) surface circulation at 5 m depth in the northern and central Adriatic driven by the spatially and temporally uniform southeasterly (scirocco) winds (Experiment 1). The winds stress is imposed along the y-axis of the model domain. (b) Same as in Fig. 3a, except for the 20 m depth.

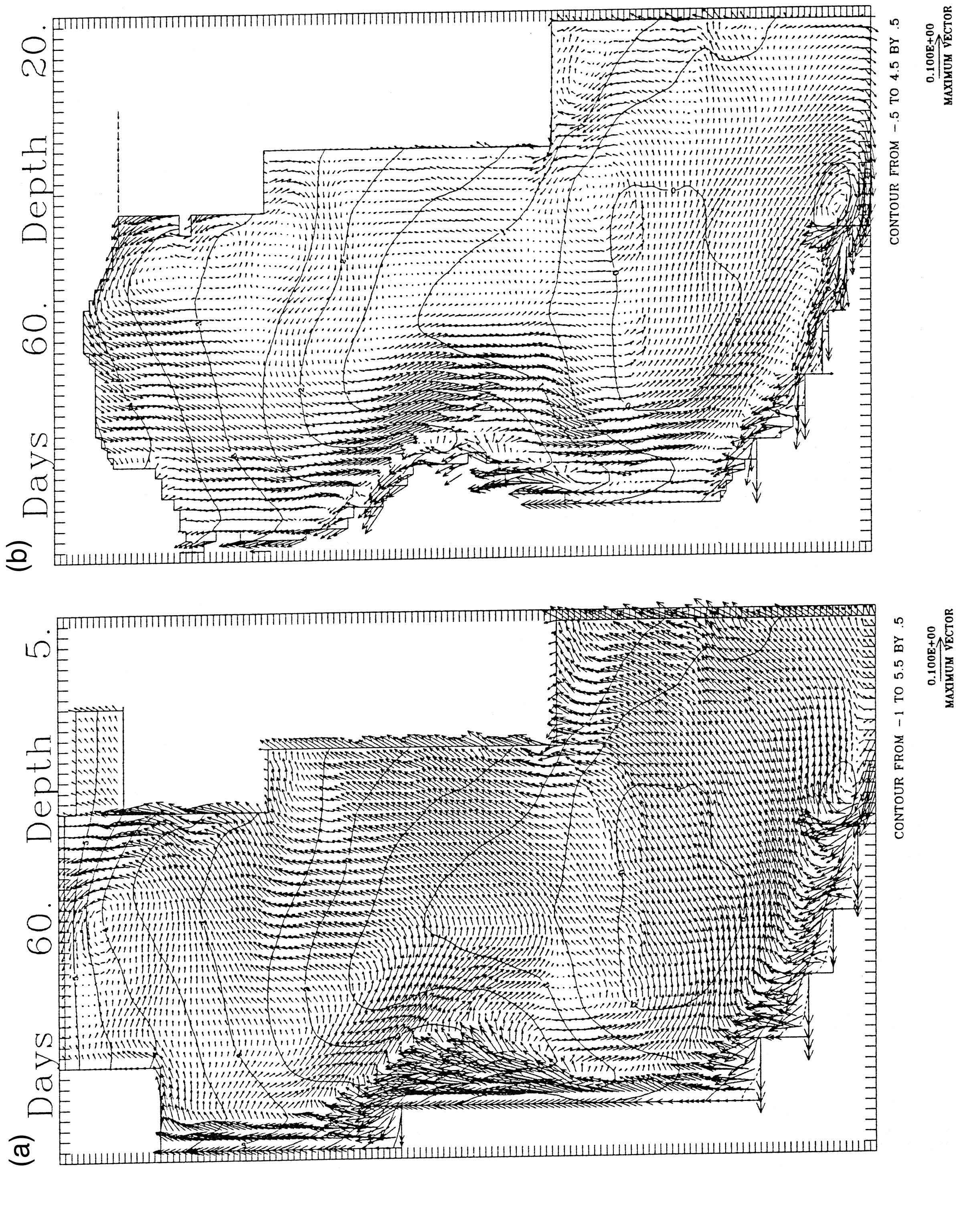
(b)
Days 60. Depth 20.
CONTOUR FROM -.5 TO 4.5 BY .5
0.100E+00
MAXIMUM VECTOR
(a)
Days 60. Depth 5.
CONTOUR FROM -1 TO 5.5 BY .5
0.100E+00
MAXIMUM VECTOR

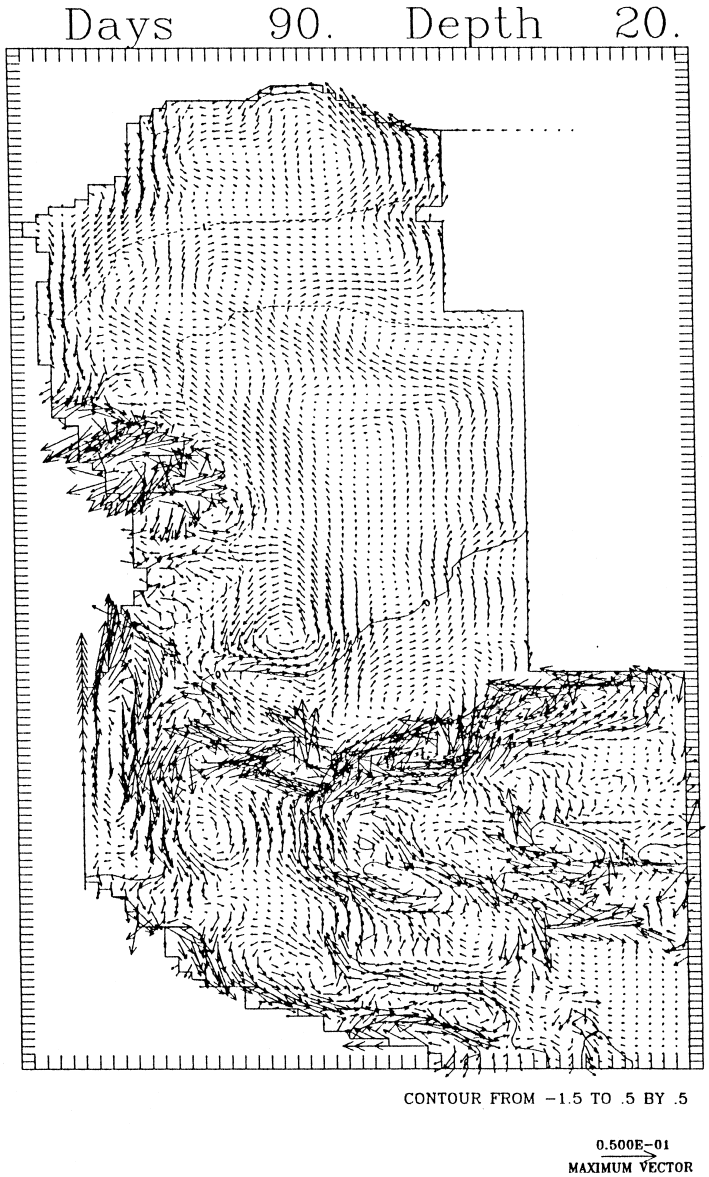

Fig. 4. Circulation pattern at 20 m depth in response to 90 days of uniform cooling of 80 W/m^2 over the basin (Experiment 2).

many features of the surface currents are different from the depth-averaged circulation, and reflect the direct response to the scirocco winds.

The circulation tends to modify at the deeper levels, as the topographic torque has a stronger effect on the flow. At 20 m depth, the circulation shows a

Fig. 5. (a) Density distribution at 20 m depth in response to 90 days of uniform cooling of 80 W/m^2 over the basin (Experiment 2). (b) Density transect along the axis of the basin for Experiment 2. (The section crosses the western through the Jabuka Pit).

(a)

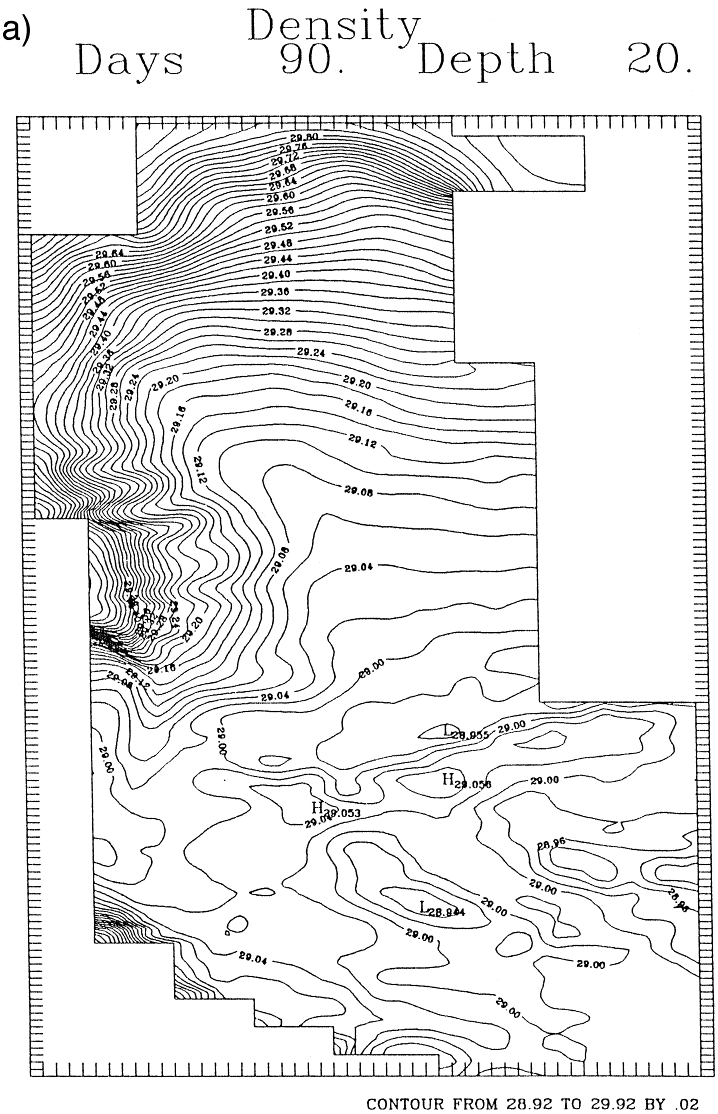
Density
Days 90. Depth 20.
CONTOUR FROM 28.92 TO 29.92 BY .02

(b)

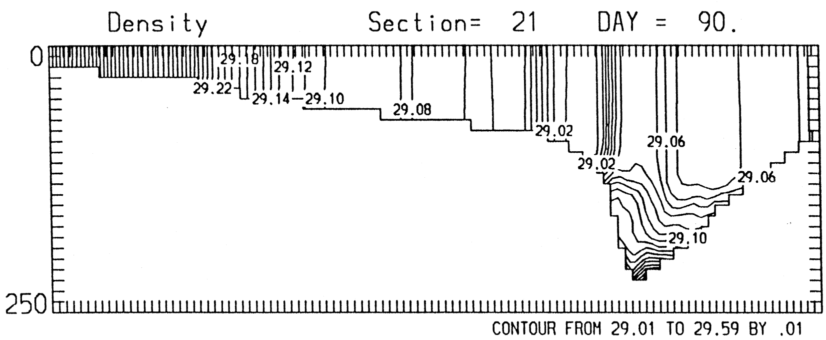
Density Section= 21 DAY = 90.
0
250
CONTOUR FROM 29.01 TO 29.59 BY .01

basinwide cyclonic cell with northerly currents along the east coast and southerlies on the Italian side (Fig. 3b). The northward flowing jet along the Italian coast is weaker and narrower, and is separated by the southward flow by anticyclonic eddies. The southward flowing rim current has a typical speed of 10 cm/s and bifurcates in the central basin; part of it continues to flow south–southeastward and leaves the basin from the open boundary, whereas the second branch flows eastward in the central basin. This latter current turns cyclonically along the Croatian coast and forms a weaker, meandering rim current along the east coast. Four distinct anticyclonic eddies of different sizes are identified here. The largest of these is located to the north of the 50 m isobath where the flow turns northwestward following the topographic slope and eventually meets the rim current of the opposite coast. The broader, basin-wide cyclonic loop of the circulation is closed by the current meander between the cyclonic–anticyclonic eddy pair situated near the northeast corner of the basin. Most of these features of the 20 m depth circulation pattern persist at deeper levels with some minor differences.

3.2. Response to thermohaline forcing only

The response of the system to climatological mean winter cooling is investigated in the second experiment. Starting from an initial state of rest, the basin is forced by the spatially and temporally uniform heat loss of 80 W/m^2 and the salt flux rate (evaporation minus precipitation, $E-P$) of 3 mm/day for a period of 90 days. These values are estimated by taking an average of the 5 month long data from November to March given by Picco (1991). The 20 m circulation pattern that developed during the 90 days forcing is shown in Fig. 4. The most distinguishing features of the circulation are the ubiquitous mesoscale eddies and complex current system formed by two cyclonic circulation cells in the central and northern basins. The circulation in the northern basin is weaker with currents having speeds no more than a few centimeters/second. It consists of a large cyclonic gyre with mesoscale eddies and complicated mid-basin current system. The interior of the gyre in the central basin consists of a series of cyclonic eddies interconnected by a topographically controlled current system. The major currents are those circulating along both sides of the sill as well as along the shelf break north of the Jabuka Pit.

The corresponding density field at 20 m depth (Fig. 5a) shows production of a significant amount of dense water in the basin, even without intensified cooling episodes associated with the northerly cold air outbreaks. It reveals pronounced lateral density gradients from shallower coastal regions towards the interior. The surface density varies from 29.8 kg/m^3 near the northern coast to about 29.00 kg/m^3 in the interior of the central basin. Comparison of the density distribution with the bathymetry given in Fig. 1b shows a significant amount of dense water with $\sigma_t > 29.2$ kg/m^3 in areas shallower than ~ 50 m. The areas deeper than 100 m (i.e., central basin) has the spatially uniform density of ~ 29.0 kg/m^3. The cross-shelf density gradients are the consequence of more rapid cooling of the shallower regions with respect to the adjacent deeper waters under the uniform cooling.

The meridional density transect along the basin (Fig. 5b) shows clearly the vertically uniform dense water within the entire water column except over the deepest part of the Jabuka Pit where the convective mixing is shown to extend up to ~ 120 m depth with the density of 29.0 kg/m^3. The water mass formed here is relatively saltier (38.5 ppt) and warmer (13.5–13.8°C) reflecting the homogenization of the subsurface MLIW water mass of the initial stratification. In the pit below 120 m, the initial stratification is however not modified as the dense water occupying the shallower northern and central parts of the basin is not dense enough to sinks to the bottom of the pit. Mixing however homogenizes the entire water column south of the pit.

3.3. Response of both scirocco wind and thermohaline forcing

The third experiment considers the circulation and thermohaline structure of the basin under combined forcing by the scirocco wind and the surface thermohaline fluxes used separately in the first two experiments. The combined forcing by the scirocco winds and the mean surface thermohaline fluxes develops a basinwide circulation system resembling a combination of those presented in Fig. 3a and Fig. 4. The

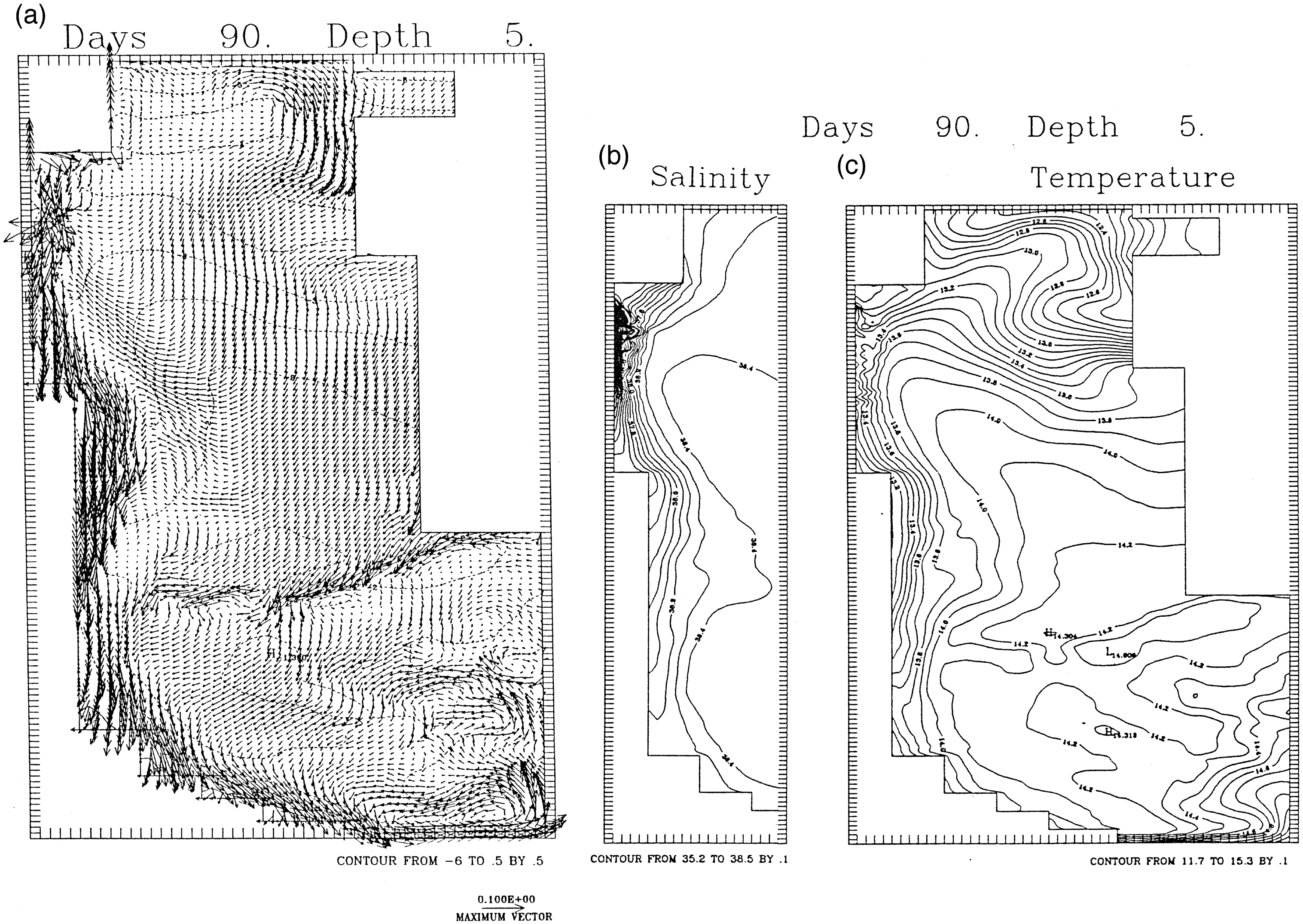

Fig. 6. (a) Circulation pattern at 5 m depth in response to 90 days of uniform cooling, scirocco winds and freshwater discharge (Experiment 4). (b) Salinity and temperature distributions at 5 m depth in response to 90 days of uniform cooling, scirocco winds and freshwater discharge (Experiment 4). Only the western part of the salinity distribution displaying the salinity front associated with the fresh water discharge is shown.

flow along the Italian coast is characterized by the counter-flowing meridional current system whose most noticeable feature is the interconnection between the northern and central basins through the southward flowing rim current. All the circulation features of the central basin are very similar to those described in Fig. 4. The surface density distribution is basically the same as in Fig. 5a and will not be discussed.

3.4. Response of scirocco wind, thermohaline forcing and fresh water discharge

The fourth experiment represents more realistic conditions for dense water mass formation and spreading characteristics in the northern and central Adriatic. The scirocco winds together with the surface thermohaline fluxes as well as the fresh water discharge from River Po are used together to drive the circulation. Once again, all these forcings are taken as temporally and spatially uniform similar to the previous experiments. The comparison of this experiment with the previous one therefore gives the contribution of River Po freshwater discharge on the mean winter circulation. The freshwater discharge is specified in the form of a point source from the coast near the northwestern corner of the model domain. It is located approximately 50 km south of the Po Delta to make it representative of all the rivers discharging to the northern part of the Italian coastline. The fresh water discharge of 1500 m^3/s added to the other forcings modifies the circulation and the thermohaline structure of the northern and central Adriatic substantially (Fig. 6a). The most striking contribution of the fresh water discharge is the generation of a pronounced southward flowing current along the Italian coastline. It is separated from the rest of the basin circulation by a broader northward reverse current which constitutes part of the anticyclonic circulation cell developed in the northern shelf region. The shelf circulation is therefore switched from cyclonic to anticyclonic by the inclusion of the fresh water discharge. A bifurcation of the fresh water induced current system takes place in the vicinity of the river mouth giving rise to two separate coastal currents flowing in opposite directions. The northward branch is a well-known feature of the river outflows and related to the potential vorticity conservation (Gill, 1976; Chao and Biocourt, 1986; Wang, 1987). This branch follows the coast turning around the northeast corner and eventually joins the interior current system. A similar structure is also observed in the northwestern shelf of the Black Sea in relation with the River Danube discharge (Oguz et al., 1995) and surface outflow of the Black sea waters from the Dardanelles Strait (Unluata et al., 1990).

Over the shelf break north of the Jabuka Pit, a current locked to the steep topographic slope crosses the basin from east to west. This zonal flow is originated by the northward flowing coastal current system along the Croatian coast but supported by the south–southwestward currents of the northern basin. This narrow jet-like current together with the currents along both the eastern and the western coasts form the cyclonic cell of the central basin. The cyclonic cell however was also present in the previous experiment, and therefore is not much affected by the fresh water-induced circulation. The buoyancy-induced flow system associated with the River Po also alters the stratification characteristics of the basin considerably. One important modification is the presence of a salinity front extending up to the central basin along the Italian coast (Fig. 6b). The other most apparent change is the development of a relatively warmer temperature field within the basin (Fig. 6c). The coolest temperatures, observed near the northern coast with about 12.5–13.0°C, are approximately 1.5–2.0°C higher than those predicted in the previous experiment. The lateral temperature gradient of about 0.5°C persists across the rim current along the Italian coast all the way to the open boundary of the basin. This gradient is associated

Fig. 7. (a) Circulation pattern at 20 m depth immediately after the CAO event, at day 75 (Experiment 5). (b) Circulation pattern at 20 m depth 15 days after the end of the CAO event and re-establishment of the uniform cooling and scirocco winds, at day 90 (Experiment 5). (c) Circulation pattern at 20 m depth 30 days after the end of the uniform cooling, but with scirocco winds and fresh water discharge, at day 120 (Experiment 5). (d) Near-bottom circulation (along l3th sigma surface) developed immediately after the CAO event, at day 75 (Experiment 5).

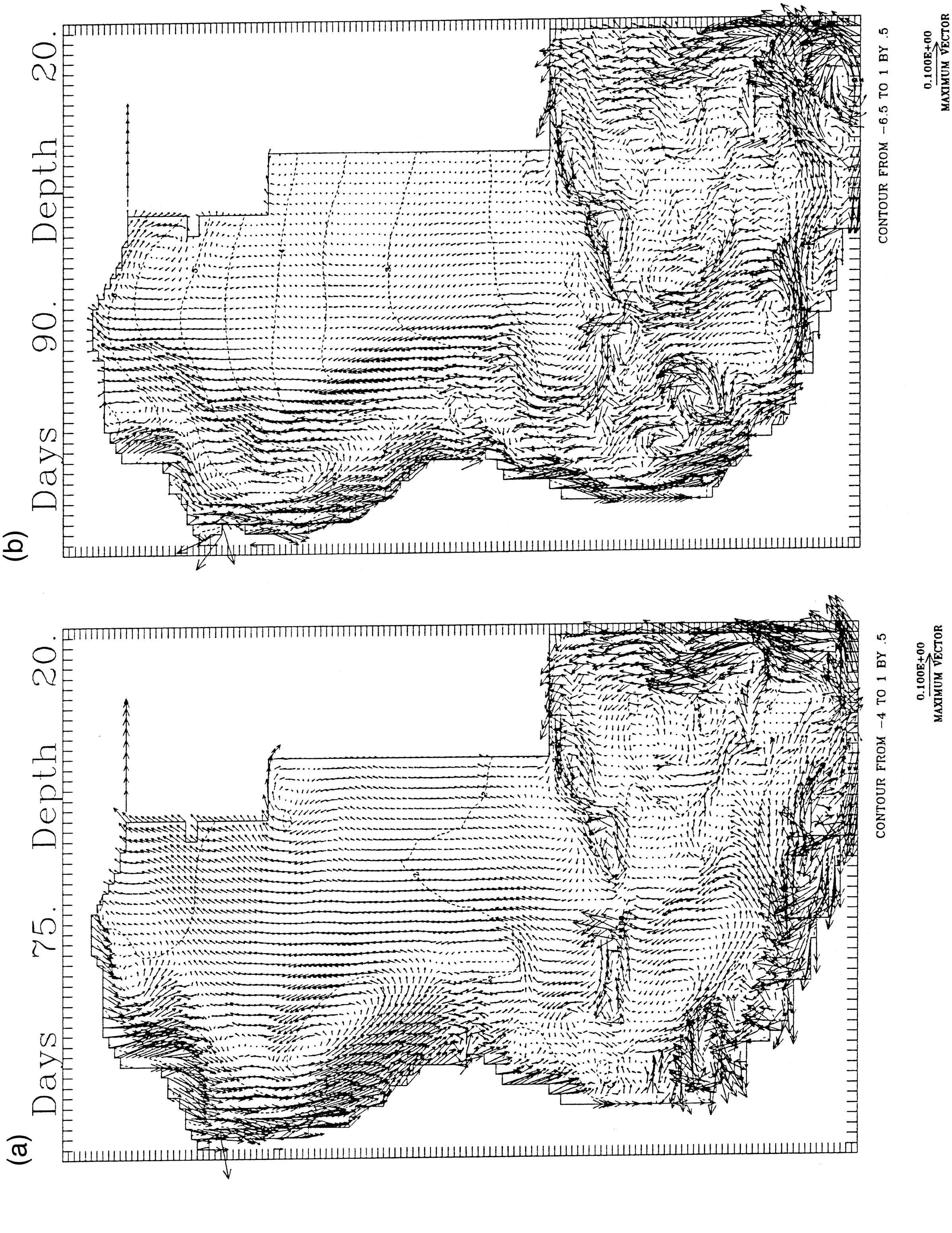
(b)
Days 90. Depth 20.
CONTOUR FROM −6.5 TO 1 BY .5
0.100E+00
MAXIMUM VECTOR
(a)
Days 75. Depth 20.
CONTOUR FROM −4 TO 1 BY .5
0.100E+00
MAXIMUM VECTOR

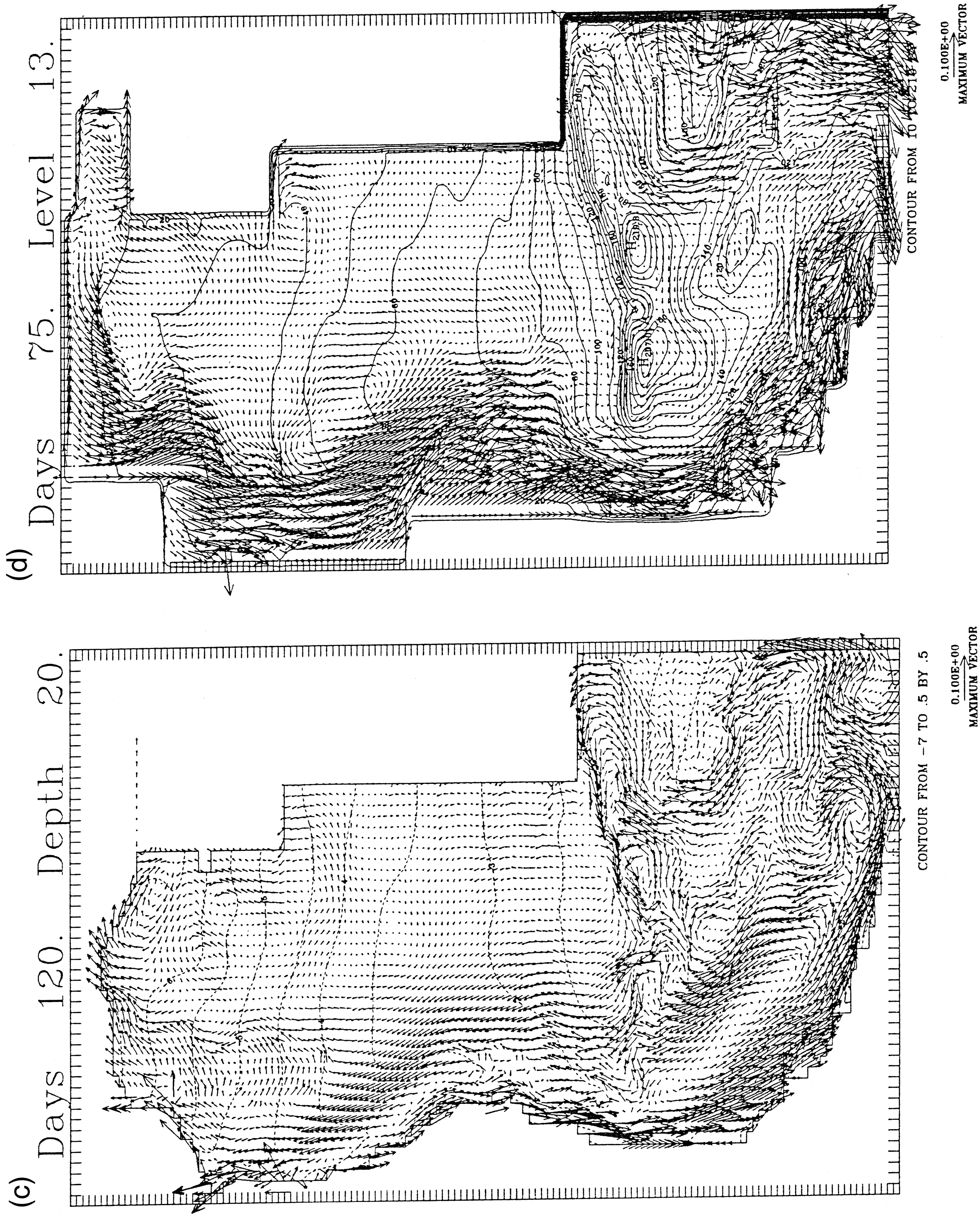

Fig. 7 (continued).

with a similarly strong salinity gradient, particularly intense near the discharge region. This rim current frontal zone resembles those observed from the AVHRR imagery (Barale et al., 1984) as well as from the CZCS pictures (Sturm et al., 1992).

Instead of the strong lateral variability in the temperature and salinity distributions near the fresh water discharge area and the northern basin in general, the rest of the basin is characterized by rather uniform distributions, typically in the range of 14.0–14.3°C for temperature and 38.4 ppt for salinity. These water mass characteristics lead to the development of a relatively less dense water mass in the basin. Comparison of the day 90 density transects with those of the previous experiment shows a typical density difference of the order of 0.2 kg/m^3 at the northern end, decreasing to 0.1 kg/m^3 towards the south. An important consequence of the fresh water induced circulation is therefore the development of even shallower convection in the central

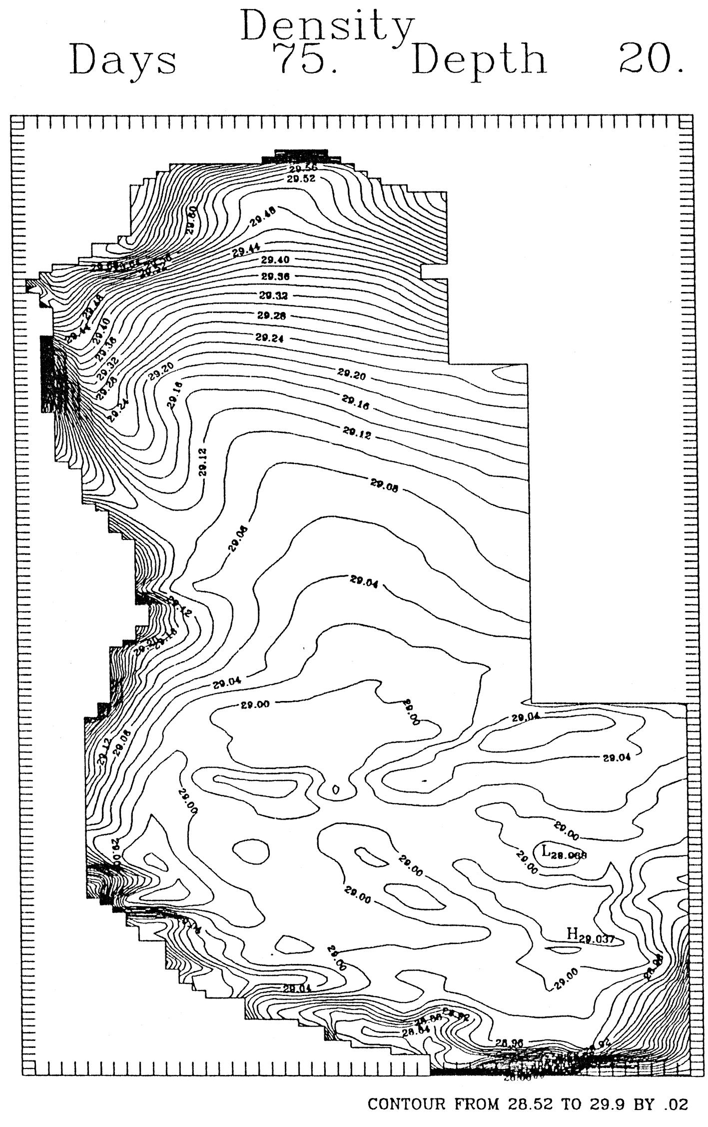

Fig. 8. Density distribution at 20 m depth immediately after the CAO event, at day 75 (Experiment 5).

basin. For example, the convective depth is about 30 m shallower over the Jabuka Pit, and the coastal density front extends all the way to the bottom.

3.5. Response of CAO outbreaks

In the fifth and sixth experiments, the effect of continental air outbreaks (CAO) in generating the dense water mass formation is simulated by a pulse of bora winds and intense surface cooling. After 60 days of simulations under the forcings of the previous experiment, the CAO pulse is applied for a duration of two weeks. The cooling is increased linearly from its background value of 40 W/m^2 (half of its value used in the previous experiments) to the maximum value of 400 W/m^2 within its first 2 days. The maximum cooling prevails for the next 10 days and then decreases linearly to the background value of 40 W/m^2 again within the last 3 days of the CAO outbreak. $(E-P)$ rate is kept at its background value of 3 mm/day during this period, for simplicity. As the scirocco winds of 0.5 dyn/cm^2 are stopped at day 60, the bora winds are switched on and increased to a maximum value of 1.2 dyn/cm^2 within the next 3 days. After 10 days of strong winds with this intensity, they diminish linearly from day 72 to 75 corresponding to the last 3 days of the CAO episode. The conditions prior to the CAO are then imposed again. The scirocco winds are kept until the end of the integration period (day 120) whereas the background cooling is turned off 15 days later, at day 90. The evolution of the system is monitored within the last 30 days when the system is driven by the combination of the fresh water discharge and steady scirocco winds. The CAO experiment is repeated with the modification in the initial stratification of the water column at depths greater than $\sim$ 150 m. Then, the profiles shown by the broken lines in Fig. 2 are used as the initial conditions.

The strong bora winds and intense cooling prescribed for a period of 2 weeks introduces substantial transients in the flow field and the dense water mass formation characteristics. At day 60, just before the CAO pulse starts affecting the basin, the circulation is similar to the one described in the previous experiment. However, at the end of the pulse (i.e., day 75), the horizontal circulation pattern is seen to have undergone considerable modification (Fig. 7a). The major change is the intensification and widening of the fresh water induced coastal jet in the northern basin. The broader reverse flow adjacent to it has disappeared, and the anticyclonic tendency of the northern basin circulation is shifted to cyclonic. The coastal jet is weakened near Ancona, where it deflects cyclonically to form the north–northwestward currents of the northern basin. Further south, between Ancona and Pescara, a weak coastal current system is present and interacts with the central basin circulation through a series of small scale eddies. The central basin circulation is cyclonic and similar to that of the previous experiment, except for the intense meandering of the coastal current and associated anticyclonic eddies. The interior of the gyre has considerable mesoscale activity and again shows a strong signature of topographic steering, described before.

The circulation pattern at day 90 (Fig. 7b) describes the motion 15 days after the termination of the bora episode in response to the steady scirocco winds and the fresh water discharge. The coastal jet along the Italian side has a more organized shape and a well-defined structure all the way to the open boundary. The opposite flowing current system also attains a well-defined structure throughout the northern interior. As compared to the strong currents of the western half of the northern basin, the eastern half is characterized by weak northerly currents. Ten days after the scirocco winds are stopped, the circulation (Fig. 7c) is still very similar to the day 90 pattern with a more pronounced interior northerly current reaching up to the northern coast. This flow system stays almost steady until the end of integration period.

Fig. 9. Density transects along the Pescara across the deepest of the Jabuka Pit, showing the evolution of the dense water mass formation in the central basin at (a) day 60, before the CAO event, (b) day 75, immediately after the CAO event, (c) day 90, 15 days after termination of the CAO event and re-establishment of the uniform cooling and scirocco winds, (d) day 120, 30 days after termination of the uniform cooling, but with scirocco wind and fresh water discharge.

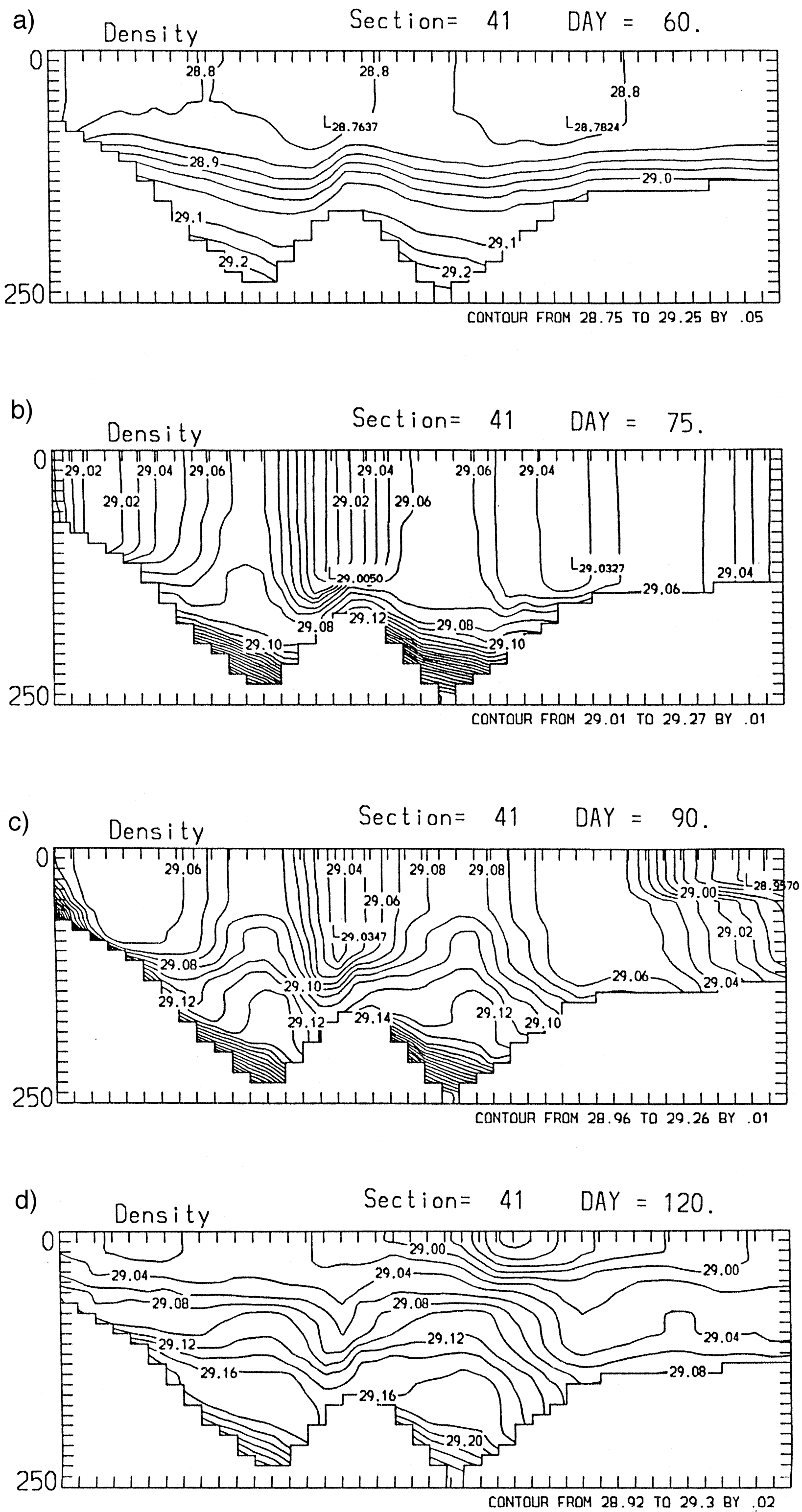
a)
Density
Section= 41 DAY = 60.
0
250
28.8
28.8
28.8
28.7637
28.7824
28.9
29.0
29.1
29.1
29.2
29.2
CONTOUR FROM 28.75 TO 29.25 BY .05
b)
Density
Section= 41 DAY = 75.
0
250
29.02
29.04
29.06
29.02
29.04
29.02
29.06
29.06
29.04
29.0050
29.0327
29.06
29.04
29.08
29.12
29.08
29.10
29.10
CONTOUR FROM 29.01 TO 29.27 BY .01
c)
Density
Section= 41 DAY = 90.
0
250
29.06
29.04
29.08
29.08
29.06
29.0347
29.00
29.02
29.08
29.10
29.06
29.04
29.12
29.12
29.14
29.12
29.10
CONTOUR FROM 28.96 TO 29.26 BY .01
d)
Density
Section= 41 DAY = 120.
0
250
29.00
29.04
29.04
29.00
29.08
29.08
29.12
29.12
29.04
29.16
29.08
29.16
29.20
CONTOUR FROM 28.92 TO 29.3 BY .02

The circulation near the bottom of the basin at day 75 is shown in Fig. 7d. When compared with the surface layer circulation shown in Fig. 7a, the near-bottom circulation in the central basin represents two major changes. The first one is the broadening and intensification of the southerly current along the Italian coastline that remains equally strong south of Ancona. This current transports the dense water masses of the northern basin to the south. The second is the reversal of circulation to anticyclonic, implying that the cyclonic zonally-elongated gyre over the Jabuka Pit is replaced by a weaker anticy-

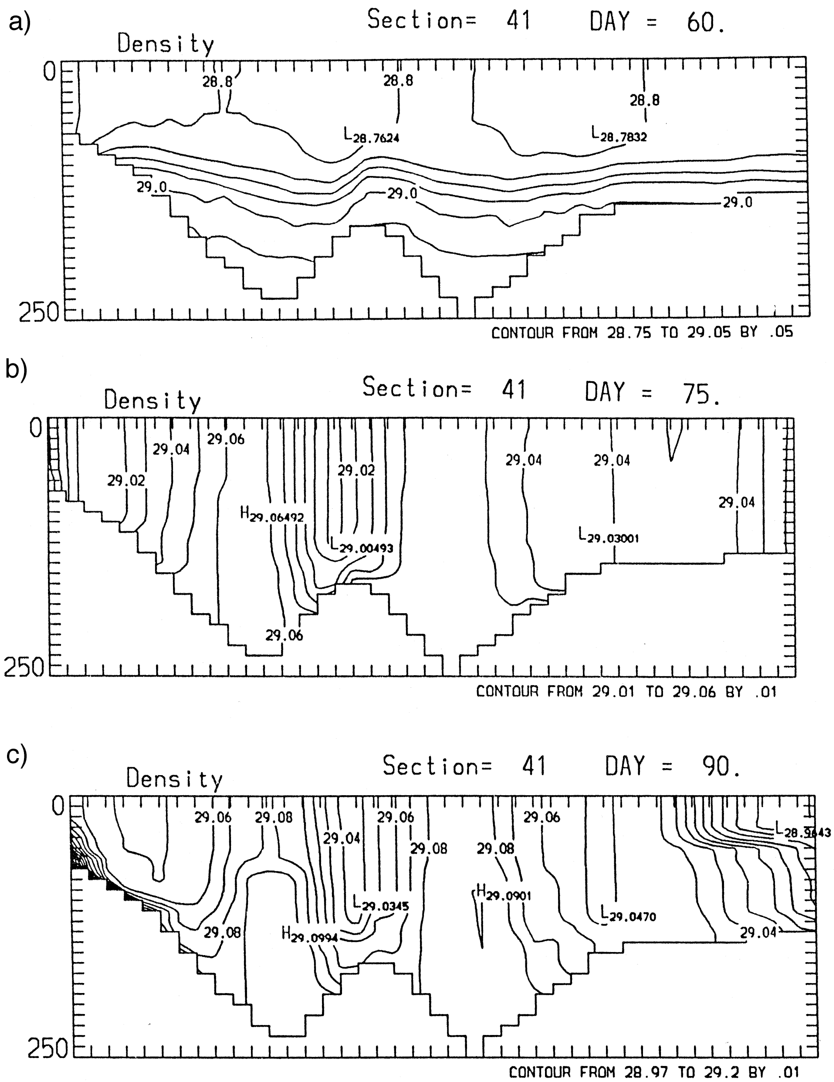

Fig. 10. Density transects along the Pescara across the deepest of the Jabuka Pit. This figure is similar to Fig. 9, except using the 'type 2' initial stratification (Experiment 6). The evolution of the dense water mass formation in the central basin is shown at (a) day 60, before the CAO event, (b) day 75, immediately after the CAO event, (c) day 90, 15 days after termination of the CAO event and re-establishment of the uniform cooling and scirocco winds, (d) day 105, 15 days after termination of the uniform cooling, but with scirocco wind and fresh water discharge. (e) day 120, 30 days after termination of the uniform cooling, but with scirocco wind and fresh water discharge.

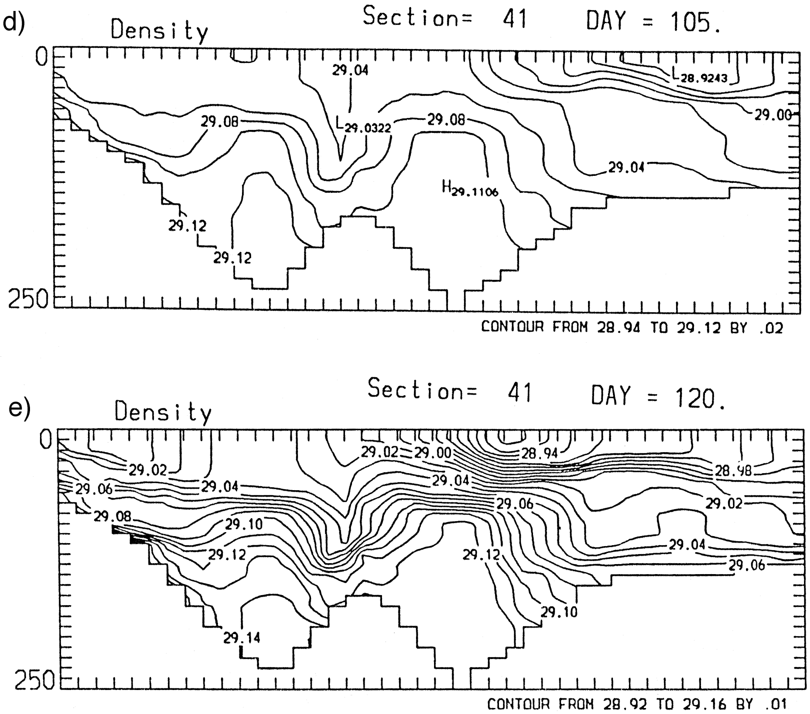

Fig. 10 (continued).

clonic gyre near the bottom. The main part of the subsurface flow exits from the basin by the meandering coastal current along the eastern coast.

A short duration intense cooling episode is sufficient for a dense water mass formation inside the basin. The 20 m density distribution (Fig. 8) is similar to the uniform and continuous cooling case, except along the northern part of the Italian coast where the fresh water dilution now present reduces slightly the density of the water mass formed on the shelf. Once again, the central basin shows a horizontally uniform density pattern with $\sigma_t \sim 29.0$ kg/m^3.

Along the cross-section off Pescara, different stages of the dense water mass formation process during the 120 days of integration period are shown in Fig. 9. The 60 days continual cooling with the intensity of 40 W/m^2 is able to generate only a shallow convection about 80 m deep with the density of 28.8 kg/m^3 ($S \sim 38.45$ ppt, $T \sim 14.4$°C), which is limited below by the strong seasonal pycnocline (Fig. 9a). At the end of 15 days intense cooling associated with the CAO, the convective overturning extends to depths of 130–150 m with a typical density of about 29.06 kg/m^3 ($S \sim 38.50$ ppt, $T \sim$ 13.4°C) (Fig. 9b). Once the intense cooling is stopped at day 75, the weak cooling of 40 W/m^2 following the CAO episode makes the intermediate water over the pits a little denser. One month later (day 120), after the cooling stopped at day 90, the mixed layer is destroyed completely (Fig. 9d) by the horizontal circulation near the surface levels (upper 50 m) advecting lighter waters over the top of the pits. Considerable temperature and salinity stratifications are established even in the absence of the vernal warming from the surface. This might be the mechanism for the strong stratification observed in the Pescara transect during the end of March 1987 (Artegiani et al., 1993).

The same experiment is repeated with a slightly different initial stratification shown in Fig. 2 with the broken lines. The new stratification allows for a weaker density gradient between the intermediate and deep waters of the Jabuka Pit and represents different inflow conditions from the southern basin prior to the beginning of the intense cooling season. The evolution of the dense water mass within the Pit is shown by a series of density transects in Fig. 10. The density structure at day 60 is similar to the previous case (Fig. 10a). The convection is limited by the subsurface density gradient level which is however weaker by about 0.15 kg/m^3 as compared to the previous case. By the end of the CAO period, contrary to the intermediate depth convection of the previous case, the convection process affects the entire water column down to the bottom, giving rise to a homogeneous water mass characterized by values of $\sigma_t \sim 29.00$–29.05 kg/m^3, S $\sim$ 38.45–38.50 ppt and T $\sim$ 13.3–13.5°C (Fig. 10b). On the other hand, the water over the ridge separating the pits is less dense those in the pits. This is due to continual replacement of waters along the ridge with less dense waters carried into the region by the local current system shown before in Fig. 7c.

The density of the vertically homogeneous layer over the pits increases slightly during the subsequent 2 weeks of weak cooling. Following the termination of the cooling, the vertical stratification is established within the water column (Fig. 10d,e).

The last two experiments imply that the extent of convection in the Pit is closely related with the stratification characteristics of the water column more than with the intensity of the surface cooling. When a relatively strong subsurface stratification exists between the MLIW at the intermediate depths and the NADW at deepest levels, a typical cooling event may not be sufficient to generate dense water mass sinking all the way to the bottom. In this case, the intermediate depth convection takes place with the vertical mixing extending only to the depth level of the strongest subsurface density gradient. In the case of weaker density gradients between these two water masses, however, the convection may extend to the bottom of the Pit. The observations performed during 15–18 February 1977 and 2–9 March 1982 (Ovchinnikov et al., 1985) give examples for such two different convective scenarios in the Jabuka Pit region. Autumn stratification characteristics are therefore crucial in determining the vertical penetration of convection and the eventual dense water mass characteristics in the central basin.

4. Conclusions

In this paper, we have attempted to provide a quantitative explanation and answers to some of the still unresolved or poorly understood dynamical issues related to the general circulation of the northern and central Adriatic Sea. Here, different forcing mechanisms interact in a complex manner in driving the basin circulation and in the wintertime production of dense water, the so-called Northern Adriatic Dense Water (NADW), over the northernmost part constituted entirely by the continental shelf. Winter convection appears to occur also in the central basin, over the Jabuka Pit $\sim$250 m deep, even though convection here does not always reach the bottom. We have addressed these issues in the context of the dynamical framework provided by a sophisticated primitive equation numerical model adapted to the somewhat idealized geometry of the northern and central Adriatic. We have carried out a series of numerical experiments examining the importance of the different forcing mechanisms, first in isolation and then combined together, with different spatial and temporal distributions to provide answers to the four major questions that constitute the scientific objectives of this work.

The first question relates to understanding the effects of the major driving mechanisms, i.e., different wind stress fields, surface fluxes and river discharge, on the basin circulation. We want also to establish which of these are crucial in producing the observed circulation pattern. Steady southeasterly winds (scirocco) produce a surface cyclonic circulation pattern all over the basin. Along the western Italian side over the shelf and continental slope, there is a surface current flowing northward in the opposite direction to what is observed. Different branches successively detach and feed the basin interior, forming the broad cyclonic gyre with a northward flow along the Croatian coast that closes the gyre in the northernmost extremity. Uniform cooling alone induces a rather weak, eddy dominated circulation pattern with no recognizable overall structure that is strongly topographically controlled. In fact the density field produced at 20 m depth (Fig. 5a) is practically identical to the pattern of isobaths (Fig. 1b). Adding the freshwater discharge concentrated in the northwestern corner to the uniform forcing of southeasterly winds reverses the coastal current along the Italian side. This now constitutes a strong jet flowing southward over the shelf and slope topography. The interior circulation of the northern basin is anticyclonic with a broad southward flow along the Croatian coast. The anticyclonic nature of the northern basin circulation is however not supported by the observations which suggest northward currents along the east coast with subsequent cyclonic circulation. One of the mechanisms which reverse the northern basin circulation to a more reasonable cyclonic one is the bora winds from the northeast. The other mechanism, which has not been included intentionally in the present model, is the continuous inflow from the southern basin along the eastern coast, which partially recirculates in the central basin, and partially proceeds northwards along the Croatian coast.

The bora winds and associated cold air outbreaks (CAO) occur during January and February, lasting for periods of 10–15 days. In experiments 5 and 6, after 60 days of southeasterly wind forcing together with the freshwater discharge, a CAO pulse is applied for 2 weeks. The resulting circulation at the end of the outbreak has a fairly realistic pattern, consistent with observations, formed by a strong southward flowing jet confined to the shelf and continental slope along the Italian side. The northern basin is comprised of an overall cyclonic gyre closed by west–northwestward currents in the deeper of the northern shelf. The central basin also exhibits a cyclonic circulation with a rather complex eddy activity. This general pattern of northern and central basin circulations also characterizes the current structure at depths.

The second issue addressed was under what conditions the convection extends to the bottom of the central Jabuka Pit. In experiments 5 and 6, it is shown that the intense cooling of 1 to 2 weeks associated with the CAO event gives rise to the formation of the NADW occupying the entire northern shelf with a uniformly mixed water column down to the bottom. However, the extent of convection within the Jabuka Pit depends on the vertical stratification characteristics prior to the onset of the cooling season. Strong subsurface stratification between MLIW and NADW within the intermediate and near-bottom layers of the pit (initial profile 'type 1' in Fig. 2) prevents deep convection. This can reach the bottom of the pit (~ 250 m) only under very strong cooling events (~ 1000 W/m^2) persisting on the region for several days, or several successive cooling events with ~ 400 W/m^2 that make the surface waters of the pit eventually denser than ~ 29.15 kg/m^3.

The third question was concerned with the relative roles of the rim current of the Italian coast versus the other components of the circulation in distributing the NADW within the basin. The strong top-to-bottom density front developed across the shelf break restricts the distribution of the dense northern water mass to the interior of the Jabuka Pit. The major part of the NADW flows persistently southward along the Italian continental slope as a vein of underflow. If the NADW produced in the CAO event is denser than the older water mass adjacent to it inside the pit at the same level, it can then cross the local isobaths and intrude below the older water mass. The other way for the spreading of this water mass inside the basin and its penetration to the deepest part of the pit is the deformation of the density front during the spring season. The third mechanism, which is not effective in our model, is the eddy-induced cross-isobath transport associated with instabilities of the density front. This mechanism has been shown to be very efficient for transporting dense water mass formed over the Arctic shelf (Gawarkiewicz and Chapman, 1995).

Acknowledgements

This work was initiated when T. Oguz and P. Malanotte-Rizzoli visited the ISDGM-CNR, Venice during October 1994. T. Oguz acknowledges the financial support provided by the CNR and thanks Director F. Dalla Porta, and other members of the Institute for their warm hospitality. This work was also supported by the National Science Foundation of the US, Grant OCE-9403471 (P. Malanotte-Rizzoli).

References

Artegiani, A., Salusti, E., 1987. Field observations of the flow of dense water on the bottom of the Adriatic Sea during the winter of 1981. Oceanologica Acta 10, 387–391.

Artegiani, A., Azzolini, R., Salusti, E., 1989. On the dense water in the Adriatic Sea. Oceanologica Acta 10, 387–391.

Artegiani, A., Gacic, M., Michelato, A., Kovacevic, V., Russo, A., Paschini, E., Scarazzato, P., Smircic, A., 1993. The Adriatic Sea hydrography and circulation in spring and autumn (1985–1987). Deep Sea Res. II 40, 1143–1180.

Barale, V., Malanotte-Rizzoli, P., Hendershott, M., 1984. Remotely sensing the surface dynamics of the Adriatic Sea. Deep Sea Res. 31, 1433–1459.

Bignami, F., Salusti, E., Schiarini, S., 1990. Observations on a bottom vein of dense water in the Southern Adriatic and Ionian Seas. J. Geophys. Res. 95, 7294–7295.

Bone, M., 1993. Development of a nonlinear levels model and its application to bora-driven circulation on the Adriatic Shelf. Estuarine, Coastal and Shelf Science 37, 475–496.

Chao, S.L., Biocourt, W., 1986. Onset of estuarine plume. J. Phys. Oceanogr. 16, 2137–2149.

Hendershott, M.C., Rizzoli, P., 1976. The winter circulation of the Adriatic Sea. Deep Sea Res. 23, 353–370.

Gawarkiewicz, G., Chapman, D., 1995. A numerical study of dense water formation and transport on a shallow, sloping continental shelf. J. Geophys. Res. 100, 4489–4507.

Gill, A.G., 1976. Adjustment under gravity in a rotating channel. J. Fluid Mech. 11, 603–621.

Killworth, P.H., 1983. Deep convection in the world ocean. Rev. Geophys. Space Phys. 21, 1–26.

Kuzmic, M., Orlic, M., Karabeg, M., Jeftic, L., 1985. An investigation of wind-driven topographically controlled motions in the northern Adriatic. Estuarine, Coastal and Shelf Science 21, 481–499.

Malanotte-Rizzoli, P., 1991. The northern Adriatic Sea as a prototype of convection and water mass formation on the continental shelf. In: Chu, P.C., Gascard, J.C. (Eds.), Deep Convection and Deep Water Formation in the Oceans. Elsevier, pp. 229–239.

Malanotte-Rizzoli, P., Bergamasco, A., 1983. The dynamics of the coastal region of the northern Adriatic Sea. J. Phys. Oceanogr. 13, 1105–1130.

Mellor, G.L. , 1990. User's guide for a three dimensional, primitive equation, numerical model. Prog. in Atmosp. and Ocean Sci. Princeton University, 35 pp.

Mellor, G.L., Yamada, T., 1982. Development of a turbulence closure model for geophysical fluid problems. Rev. Geophys. Space Phys. 20, 851–875.

Oguz, T., Malanotte-Rizzoli, P., Aubrey, D.G., 1995. Wind and thermohaline circulation of the Black Sea driven by yearly mean climatological forcing. J. Geophys. Res. 100, 6845–6863.

Orlic, M., Gacic, M., La Violette, P., 1992. The currents and circulation of the Adriatic Sea. Oceanologica Acta 15, 109–124.

Orlic, M., Kuzmic, M., Pasaric, Z., 1994. Response of the Adriatic Sea to the bora and scirocco forcing. Cont. Shelf Res. 14, 91–116.

Ovchinnikov, I.M., Zats, V.I., Krivosheya, V.G., Udodov, A.I., 1985. A formation of deep eastern Mediterranean water in the Adriatic Sea. Oceanology 25, 911–917.

Paschini, E., Artegiani, A., Pinardi, N., 1993. The mesoscale eddy field of the Middle Adriatic Sea during fall 1988. Deep Sea Res. 40.

Picco, P. (1991) Evaporation and heat exchanges between the sea and the atmosphere in the Gulf of Trieste during 1988. I1 Nuovo Cimento, 14, 335–345.

Pinardi, N., 1995. Mediterranean eddy resolving and interdisciplinary studies. CEE-MAST Second Mast days and EUROMAR market, 7–10 Nov., 1995. Project Reports V.1, pp. 433–453.

Pollak, M.I., 1951. The sources of deep water in the eastern Mediterranean Sea. J. Mar. Res. 10, 128–152.

Roether, W., Schlitzer, R., 1991. Eastern Mediterranean deep water renewal on the basis of CFM and tritium data. Dynamics of Atmospheres and Oceans 15, 333–354.

Schlitzer, R., Roether, W., Oster, H., Junghans, H.G., Hausmann, M., Johannsen, H., Michelato, A., 1991. Chlorofluoromethane and oxygen in the Eastern Mediterranean. Deep Sea Res. 38, 1531–1551.

Sturm, B., Kuzmic, M., Orlic, M., 1992. An evaluation and interpretation of CZCS-derived patterns of the Adriatic shelf. Oceanologica Acta 15, 13–23.

Unluata, U., Oguz, T., Latif, M.A., Ozsoy, E., 1990. On the physical oceanography of the Turkish straits. In: Pratt, L.J. (Ed.), The Physical Oceanography of Sea Straits. NATO ASI Ser. Kluwer Academic, Norwell, MA, pp. 25–60.

Wang, D.P., 1987. The strait surface outflow. J. Geophys. Res. 92, 10807–10825.

Zavaterelli, M., Mellor, G.L., 1995. A numerical study of the Mediterranean Sea circulation. J. Phys. Oceanogr. 25, 1384–1414.